

Galaxy Pairs in the Sloan Digital Sky Survey - III: Evidence of Induced Star Formation from Optical Colours.

David R. Patton¹, Sara L. Ellison², Luc Simard³, Alan W. McConnachie³, J. Trevor Mendel²

¹ *Department of Physics & Astronomy, Trent University, 1600 West Bank Drive, Peterborough, Ontario, K9J 7B8, Canada.*

² *Department of Physics and Astronomy, University of Victoria, Victoria, British Columbia, V8P 1A1, Canada.*

³ *National Research Council of Canada, Herzberg Institute of Astrophysics, 5071 West Saanich Road, Victoria, British Columbia, V9E 2E7, Canada*

Accepted for publication in MNRAS on October 27, 2010.

ABSTRACT

We have assembled a large, high quality catalogue of galaxy colours from the Sloan Digital Sky Survey Data Release 7, and have identified 21,347 galaxies in pairs spanning a range of projected separations ($r_p < 80 h_{70}^{-1}$ kpc), relative velocities ($\Delta v < 10,000$ km s⁻¹, which includes projected pairs that are essential for quality control), and stellar mass ratios (from 1:10 to 10:1). We find that the red fraction of galaxies in pairs is higher than that of a control sample matched in stellar mass and redshift, and demonstrate that this difference is likely due to the fact that galaxy pairs reside in higher density environments than non-paired galaxies. We detect clear signs of interaction-induced star formation within the blue galaxies in pairs, as evidenced by a higher fraction of extremely blue galaxies, along with blueward offsets between the colours of paired versus control galaxies. These signs are strongest in close pairs ($r_p < 30 h_{70}^{-1}$ kpc and $\Delta v < 200$ km s⁻¹), diminish for more widely separated pairs ($r_p > 60 h_{70}^{-1}$ kpc and $\Delta v < 200$ km s⁻¹) and disappear for close projected pairs ($r_p < 30 h_{70}^{-1}$ kpc and $\Delta v > 3000$ km s⁻¹). These effects are also stronger in central (fibre) colours than in global colours, and are found primarily in low- to medium-density environments. Conversely, no such trends are seen in red galaxies, apart from a small reddening at small separations which may result from residual errors with photometry in crowded fields. When interpreted in conjunction with a simple model of induced starbursts, these results are consistent with a scenario in which close peri-centre passages trigger induced star formation in the centres of galaxies which are sufficiently gas rich, after which time the galaxies gradually redden as they separate and their starbursts age.

Key words: galaxies: evolution, galaxies: interactions, galaxies: photometry

1 INTRODUCTION

Comparisons between galaxy populations throughout the redshift range of $0 < z < 1$ indicate that the red sequence has roughly doubled in mass during this timeframe, while the mass of the blue cloud is unchanged (Faber et al. 2007; Martin et al. 2007; Ruhland et al. 2009). The red sequence gains mass from the quenching of blue galaxies, while the corresponding loss in blue cloud mass is balanced by the ongoing star formation within blue cloud galaxies. This evolution is accompanied by an order of magnitude decrease in the cosmic star formation rate (e.g., Madau et al. 1996), a transition from disc-dominated to bulge-dominated galaxies (Oesch et al. 2010; López-Sanjuan et al. 2010), a decrease in the galaxy merger rate (e.g., Lin et al. 2008), and the hierarchical buildup of massive galaxies.

Galaxy-galaxy interactions and mergers are thought to contribute to this evolution by triggering the formation of new stars, by quenching star formation in gas-rich galaxies, and by moving

galaxies up the red sequence via dry mergers (Schiminovich et al. 2007; Di Matteo et al. 2008; Skelton et al. 2009; Wild et al. 2009). Close encounters are also thought to play a role in producing a wide variety of transient astrophysical phenomena, such as quasars (Hopkins et al. 2007; Treister et al. 2010; Green et al. 2010), submillimetre galaxies (Conselice et al. 2003; Tacconi et al. 2008), luminous infrared galaxies (Wang et al. 2006; Shi et al. 2009), and ultra-luminous infrared galaxies (ULIRGs; Dasyra et al. 2008; Hou et al. 2009; Chen et al. 2010).

Larson & Tinsley (1978) provided the first clear evidence of enhanced star formation in interacting galaxies, by comparing the optical colours of morphologically peculiar galaxies to normal galaxies. In recent years, numerous lines of evidence have confirmed this finding. The level of enhancement is typically about a factor of two (e.g., Heiderman et al. 2009; Knapen & James 2009; Robaina et al. 2009), but varies depending on the types of galaxies involved (e.g., massive galaxies vs. starforming galaxies), how the interactions are identified (e.g., visual classifications

vs. presence of a close companion), how advanced the interaction/merger is, and the method used to measure the star formation (e.g., $H\alpha$ equivalent width vs. far infrared emission). A number of recent studies of close galaxy pairs have demonstrated that the enhancement in star formation increases as pair separation decreases (Barton et al. 2000; Lambas et al. 2003; Alonso et al. 2004; Nikolic et al. 2004; Alonso et al. 2006; Geller et al. 2006; Woods et al. 2006; Barton et al. 2007; Woods & Geller 2007; Ellison et al. 2008, 2010; Woods et al. 2010). Studying this problem in reverse reveals that galaxies which are undergoing strong star formation have an increased likelihood of having a close companion (e.g., Owers et al. 2007; Li et al. 2008). There is also evidence that recent (rather than ongoing) star formation is enhanced in interacting galaxies, from studies of E+A galaxies (Nolan et al. 2007; Yamauchi et al. 2008; Brown et al. 2009; Pracy et al. 2009), the absorption-line spectra of early type galaxies (Rogers et al. 2009), and the recent star formation histories of ULIRGs (Rodríguez Zaurín et al. 2010).

Nevertheless, many questions remain. Assessment of the relative roles of gas-rich versus gas-poor galaxies in interactions and mergers has yielded some conflicting results, due in part to the methods used to identify these systems and detect their star formation. Interacting galaxies which are identified based on morphological signs of interactions are strongly biased towards systems with large gas fractions, and these tidal disturbances remain visible for longer in gas-rich systems (Lotz et al. 2010). This issue can be avoided by identifying interacting systems via the presence of close companions. However, many such close pair studies employ star formation rate (SFR) indicators which are primarily sensitive to gas-rich galaxies (e.g., those which use nebular emission lines); low levels of enhanced star formation in gas-poor systems may therefore be overlooked. Moreover, these same SFR indicators are sensitive to relatively short-lived *ongoing* star formation, and therefore may only be able to identify signs of triggered star formation in systems which are seen very shortly after close passages. Finally, a perennial problem with studies of interacting galaxies is the question of “nature versus nurture”. That is, if one detects differences between interacting and non-interacting galaxies, it is difficult to distinguish between interaction-induced effects (such as triggered star formation) and pre-interaction differences (e.g., if interacting and non-interacting galaxies reside in different environments).

One relatively obvious way forward is to analyze the optical colours of galaxies in close pairs, and compare them to a fair sample of non-paired galaxies. Optical colours can be measured for all types of galaxies, and provide a clear method of distinguishing between gas rich and gas poor galaxies, due to the well-established bi-modality of galaxy colours (e.g., Baldry et al. 2004). In addition, induced star formation alters the colours of galaxies, and on timescales which are considerably longer than those of the starbursts themselves. However, while there have been a number of previous studies of the optical colours of galaxies in interacting/merging galaxies, they have yielded some conflicting results. The earliest studies of close galaxy pairs generally found that the colours of galaxies in close pairs are similar to field galaxies (see Patton et al. 1997, and references therein), although these studies were limited to small samples of galaxy pairs, often without redshifts. In recent years, large redshift surveys have greatly increased the yield of close spectroscopic galaxy pairs, allowing differences to emerge. De Propriis et al. (2005) find that galaxies in close pairs are bluer than galaxies in their parent sample. Other studies report an excess of both extremely blue and extremely red galaxies in close pairs (Alonso et al. 2006; Perez et al. 2009b) and visually

identified mergers (Darg et al. 2010). Interpretation of these and other results is complicated by the limited size of many close pair samples, deficiencies in the quality and size of the control samples, uncertainties about the quality of colours measured in these crowded systems, and the fact that some studies do not directly probe colour changes as a function of pair separation.

Optical colours can also provide further insight into the degree to which triggered star formation is centrally concentrated. Simulations indicate that strong interactions can cause the infall of gas onto the central regions of galaxies, triggering star formation (Mihos & Hernquist 1994; Cox et al. 2006; Di Matteo et al. 2007). This process may contribute to the growth of bulges (Barton Gillespie et al. 2003; Kannappan et al. 2009; Oesch et al. 2010), even if the interactions do not lead to mergers. Several lines of observational evidence indicate that interaction-induced star formation tends to be centrally concentrated. Bergvall et al. (2003) and Park & Choi (2009) use optical colours to infer that star formation is enhanced in the centres of interacting and merging galaxies, while Barton et al. (2000) use both optical colours and $H\alpha$ equivalent widths to reach the same conclusion in a sample of close galaxy pairs. Ellison et al. (2010) use bulge versus disc colours to infer evidence of enhanced star formation in the bulges, but not the discs, of galaxies in close pairs. Rossa et al. (2007) find that the surface brightness profiles of Toomre-sequence galaxies are consistent with the presence of newly formed stars in the centres of these merging galaxies, while Haberman et al. (2010) find a central excess of core collapse supernovae in the cores of disturbed galaxies. Evidence for the infall of gas onto the centres of galaxies comes from an offset of the luminosity-metallicity relation and mass-metallicity relation to lower metallicities in close galaxy pairs (Kewley et al. 2006; Ellison et al. 2008), and a higher proportion of strongly disturbed systems in lower metallicity galaxies (Alonso et al. 2010), and is consistent with predictions from the simulations of Rupke et al. (2010). However, there are also clear examples of galaxy-galaxy interactions which trigger off-centre star formation (Inami et al. 2010; Zhang et al. 2010) or galaxy wide star formation (Goto et al. 2008). Furthermore, Knapen & James (2009) find no excess of central star formation in a sample of galaxies with close companions, despite the overall SFRs of these galaxies being nearly twice as high as galaxies in their control sample.

We aim to shed new light on these issues by measuring the $g-r$ colours of galaxies in Sloan Digital Sky Survey (SDSS) close pairs, and comparing them with a control sample of non-paired galaxies that are matched in both stellar mass and redshift. In addition, by comparing with both wide separation pairs and close projected pairs (i.e., interlopers), we wish to tease apart colour differences which are due to interactions from those which result from environmental differences or poor photometry. Finally, by comparing global colours to central (fibre) colours, we will investigate the degree to which induced star formation is centrally concentrated. Compared with earlier studies of the colours of galaxies in close pairs, our study is unparalleled in terms of the size of the pairs sample, the quality of the photometry, the combination of global and central colours, the size and robustness of the control sample, the comparison with close projected pairs, and the use of colour offsets.

We describe the selection of our pairs and control samples in Section 2, along with our measurements of global and central colours. In Section 3, we present the overall distributions of global colours in paired galaxies, along with their dependence on pair separations and relative velocities. In Section 4, we divide our sample into four subsets (red sequence, blue cloud, extremely red, and ex-

tremely blue), and explore how the fractions and colours of galaxies in these subsets depend on projected separation. We then assess the degree to which these trends are related to central (rather than global) colours by analyzing fibre colours (§ 5). We introduce a new measure called colour offset in Section 6, and relate our findings to predictions from a simple starburst model (Section 7). We finish with our conclusions in Section 8. We adopt a concordance cosmology of $\Omega_{\Lambda} = 0.7$, $\Omega_M = 0.3$, and $H_0 = 70 \text{ km s}^{-1} \text{ Mpc}^{-1}$ throughout the paper.

2 SAMPLE SELECTION AND COLOUR MEASUREMENTS

We wish to analyze the optical colours of galaxies in close pairs, and to compare them with a control sample of galaxies which do not have close companions. In addition, we will compare close and wide pairs, in order to be certain that any effects attributed to ongoing interactions/mergers decline at wider separations, as would be expected in this scenario. Finally, we will compare close physical pairs to close projected pairs, in order to ensure that our findings are not adversely affected by poor photometry due to crowding. In this section, we describe our initial acquisition of galaxies from the SDSS Data Release 7 (hereafter DR7) of Abazajian et al. (2009), along with our selection of galaxies in pairs, and the creation of an unbiased control sample.

2.1 A Catalog of SDSS Galaxies

Studies of close pairs of galaxies have benefitted greatly from the advent of large redshift surveys. The availability of redshifts for both members of a close pair reduces the contamination due to unrelated foreground/background companions, and allows one to compare intrinsic galaxy properties as a function of projected physical separation and relative line-of-sight velocity. We therefore begin by requiring all galaxies in our sample to have secure spectroscopic redshifts from the SDSS DR7; specifically, we select galaxies from the SpecPhoto table which have $z\text{Conf} > 0.7$ (i.e., all redshifts are at least 70% secure).

We further limit our analysis to the SDSS Main Galaxy Sample (Strauss et al. 2002), by requiring extinction-corrected Petrosian apparent magnitudes of $m_r \leq 17.77$. We impose an additional limit of $m_r > 14.5$ in order to avoid the unreliable deblending of large galaxies, which can lead to single galaxies being misclassified as close pairs, triples, etc. We impose a minimum redshift of 0.01 to ensure that redshifts are primarily cosmological, and we impose a maximum redshift of 0.2 to avoid the regime of high incompleteness and poor spatial resolution. We also require all objects to be classified as galaxies both photometrically (SpecPhoto.Type=3) and spectroscopically (SpecPhoto.SpecClass=2).

Finally, studies of galaxy pairs benefit from knowledge of the luminosity or mass ratio of every pair. We therefore also require every galaxy to be included in the MPA-JHU DR7 stellar mass catalogue¹. These stellar masses were measured using fits to SDSS *ugriz* photometry (Salim et al. 2007), rather than using spectral features (Kauffmann et al. 2003), although in general these mass estimates agree very well². Together, these criteria yield a catalogue of 615,196 galaxies.

2.2 The Pairs Sample

We identify a sample of galaxy pairs following the general approach of Ellison et al. (2008). For each galaxy in the catalogue described above, we identify the closest companion satisfying the following criteria:

- (i) projected physical separation of $r_p < 80 \text{ } h_{70}^{-1} \text{ kpc}$
- (ii) line-of-sight rest-frame velocity difference of $\Delta v < 10,000 \text{ km s}^{-1}$
- (iii) stellar mass ratio (companion mass divided by host mass) of $0.1 < \text{mass ratio} < 10$

If several companions are found for a given host galaxy, the companion with the smallest r_p is selected. If no companions are found, the galaxy is designated as a potential control galaxy (see below).

Finally, following Ellison et al. (2008), we randomly remove 67.5% of galaxies which are in pairs with angular separations greater than $55''$, in order to compensate for the fact that pairs with smaller angular separations would otherwise be underrepresented in our sample. This small scale spectroscopic incompleteness results from the well known SDSS fibre collision constraint (Strauss et al. 2002), whereby one cannot simultaneously acquire spectra for two galaxies within $55''$. Thankfully, plenty of these pairs are nevertheless present in SDSS, due to overlap between adjacent plates and the use of two or more plates in some regions. Ellison et al. (2008) use the spectroscopic incompleteness measurements of Patton & Atfield (2008) to estimate that 67.5% of pairs at angular separations below $55''$ are missed as a result of these fibre collisions. We therefore exclude the same fraction of galaxies in pairs with separations $> 55''$.

Application of all of these criteria to the catalogue described in Section 2.1 yields a sample of 22,777 galaxies with a companion. Hereafter, we refer to these galaxies as “paired galaxies”.

2.3 The Control Sample

In order to ascertain how interactions/mergers affect galaxy properties, we wish to compare our sample of paired galaxies with a sample of non-interacting galaxies. However, if one simply selects galaxies at random from the remaining (non-paired) galaxies in the catalogue, the resulting distribution of stellar masses and redshifts will be significantly different from the pairs sample (Ellison et al. 2008; Perez et al. 2009a), due to the pair selection criteria, SDSS fibre collisions, etc. Given that many observed properties of galaxies are redshift dependent, and that intrinsic galaxy properties are known to correlate with stellar mass (e.g., Abbas & Sheth 2006), we therefore create a control sample that is matched to the pairs sample in both stellar mass and redshift. Unlike Ellison et al. (2010), we do not attempt to explicitly match our control sample to the environment of paired galaxies; however, we do compare the environments of paired and control galaxies in Section 4.1, and we investigate the dependence of our results on environment in Section 6.

The control sample is created by first finding the best simultaneous match in redshift and stellar mass for each paired galaxy. This yields an initial control sample which is equal in size to the paired sample, with nearly identical distributions of redshift and stellar mass. We confirm this agreement by carrying out Kolmogorov-Smirnov (K-S) tests on the two distributions, in which low significance levels would imply significantly different cumulative distribution functions; we instead find significance levels of 100.0000% in each case. We therefore increase the size of

¹ <http://www.mpa-garching.mpg.de/SDSS/>

² See http://www.mpa-garching.mpg.de/SDSS/DR7/mass_comp.html

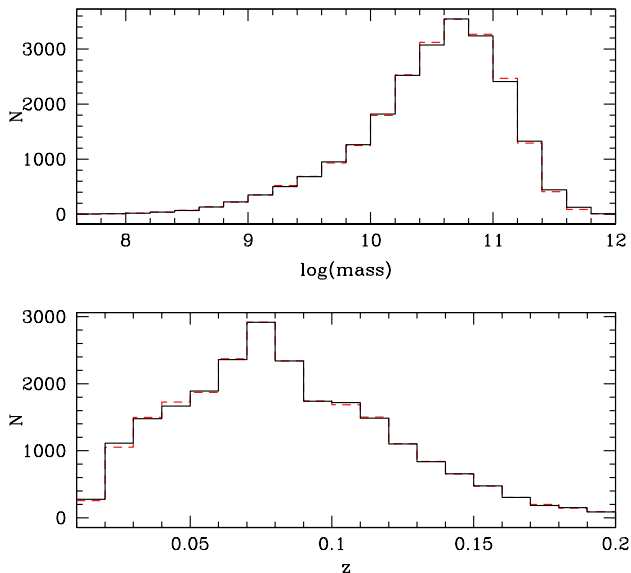


Figure 1. Histograms of redshift and stellar mass for galaxies in pairs (solid black lines) and in the control sample (dashed red lines) are used to assess the success of the control sample matching procedure. The control sample histogram has been scaled by a factor of 13, to account for the fact that each paired galaxy has 13 associated control galaxies. K-S test results are 64% and 68% for redshift and mass distributions respectively, indicating that the paired and control galaxies samples are consistent with being drawn from the same parent distributions in redshift and stellar mass.

our control sample by repeating this exercise until the distributions in redshift and stellar mass of the control sample start to diverge significantly from those of the paired sample. With this approach, we are able to create a control sample that is 13 times larger than the pairs sample. Figure 1 confirms that the resulting redshift and stellar mass histograms appear to be in excellent agreement with one another, and this impression is verified by K-S test results of 64% and 69% respectively (these values would have dropped to 11% and 27% respectively if we had included a fourteenth iteration of the matching procedure). The fact that the control sample is much larger than the pairs sample means that the control sample will make a negligible contribution to the statistical errors in our results.

We tag each control galaxy with the properties of the paired galaxy it was matched to: specifically, the projected separation r_p , the rest-frame velocity difference Δv , the stellar mass ratio, and the unique identifier (SDSS objID) of the paired galaxy. This will enable us to compare individual paired galaxies with their associated control samples, or to compare subsets of the paired sample (selected based on any combination of pair properties) with the corresponding control galaxies. Both approaches will prove to be very powerful in revealing differences in the colours of paired and control galaxies.

There are several important advantages of this approach. The first is that we are able to account for changes in redshift and/or stellar mass as a function of pair separation, Δv , etc. This can be contrasted with other published studies in which the properties of control galaxies are averaged over the full sample, rather than being computed as a function of pair separation, etc. Secondly, we can compare any individual paired galaxy to its own control sam-

ple, thereby providing an additional tool for assessing which paired galaxies are most different from their controls.

In the analysis and interpretation that follows later in this paper, the reader should keep the following two points in mind. First, any differences between galaxies in the paired and control samples cannot be due to differences in stellar mass or redshift; therefore, these differences may tell us something fundamental about how interacting galaxies differ from non-interacting galaxies. Secondly, if the properties of control sample galaxies are found to vary with pair properties (e.g., pair separation), this is likely due to variation in the stellar mass and/or redshift distribution of galaxies in the pairs sample. While both types of information are in principle useful, the latter must be treated with caution, since changes in the stellar mass and/or redshift distribution may be the result of selection effects in the pairs sample (e.g., redshift-dependent selection effects, incompleteness in the stellar mass catalog, spectroscopic incompleteness, etc.). As a result, we will focus primarily on differences between the pairs and control samples.

2.4 GIM2D Fits

In addition to satisfying the basic requirements of our pair and control sample algorithms, we now further require that all galaxies in our sample have high quality global (integrated) rest-frame $g - r$ colours measured by Simard et al. (2010). These colours were computed using the Galaxy Image 2D (GIM2D) software of Simard et al. (2002), using simultaneous g and r band fits to the SDSS images. All colours are corrected for Galactic extinction, and converted to rest-frame quantities using the k -correction software of Blanton & Roweis (2007). Simard et al. (2010) demonstrate that these fits, which were carried out using improved background subtractions and segmentation maps, provide robust colour measurements for galaxies which have close companions. This allows us to avoid known challenges with the photometry of crowded systems (e.g., Patton et al. 2005; Masjedi et al. 2006; De Propriis et al. 2007)³.

In particular, we require each galaxy in the pairs and control sample to satisfy the following criteria:

- (i) successful GIM2D simultaneous g - and r -band fit from Simard et al. (2010)
- (ii) rest-frame $g - r$ colour error less than 0.1 mag
- (iii) the fibre colour predicted by the GIM2D model fit must be within 0.1 mag of the observed SDSS fibre colour⁴
- (iv) visual inspection confirms that the object is a distinct galaxy (inspection is complete only for pairs with $r_p < 10 h_{70}^{-1}$ kpc)

Overall, 94% of galaxies in our preliminary paired and control galaxy samples satisfy all of these criteria. This yields final samples of 21,347 paired galaxies and 261,023 control galaxies⁵, with an average of 12.23 control galaxies for each paired galaxy. We note that these samples are substantially larger than those of Ellison et al. (2010), since their pairs sample is restricted to DR4 galaxies with $z < 0.1$, and their control sample is only four times

³ We investigate the importance of careful photometry in crowded fields in Section 4.4.

⁴ More precisely, the “ Δ (fibre colour)” parameter defined and reported in Simard et al. (2010) must be within 0.1 mag of the control sample mean.

⁵ In cases where a paired galaxy has been removed from the sample due to application of the above criteria, its associated control galaxies are also removed.

larger than their pairs sample (due to their additional requirement for a match on local density).

2.5 SDSS Fibre Colours

The Simard et al. (2010) catalogue contains global colours for each galaxy in our paired and control galaxy samples, measured using bulge+disc decomposition. These colours are representative of the galaxies as a whole, and should be sensitive to induced star formation that is either global or centrally concentrated. However, the SDSS database also provides measurements of fibre colours, which are measured within the central 3 arcseconds of each galaxy. We have converted these to rest-frame fibre colours using the extinction corrections from the SDSS database and the k -corrections described in the preceding section. These fibre colours provide a probe of the central star formation in each galaxy, although the degree to which these colours are non-global depends on the covering fraction (CF) of the fibres. Moreover, if we wish to compare the fibre colours of paired and control galaxies, we must ensure that they have similar covering fraction distributions.

In Figure 2, we present r -band CF histograms of paired and control galaxies. We find broadly similar distributions, with a small offset ($\sim 1.5\%$) towards larger CF's for paired galaxies. While these samples were not matched on CF, reasonable agreement is to be expected, given that each paired galaxy is matched in both redshift and stellar mass to its control galaxies⁶. The offset is in the direction expected, given that Ellison et al. (2010) report that galaxies in a subset of this pairs sample have somewhat higher bulge fractions than control galaxies. Most importantly, the offset in CF between paired and control galaxies is sufficiently small that it should have a negligible influence on the resulting colours, allowing us to make a fair comparison of fibre colours between paired and control sample galaxies.

We also note that the median CF of paired galaxies is 29%, and 96% of paired galaxies have covering fractions of less than 50%. Therefore, these fibre colours do in fact provide a good probe of central colours. Moreover, unlike the global colours of Simard et al. (2010), the fibre colours are model independent, and they are not affected by deblending problems due to close neighbouring galaxies or stars. Therefore, fibre colours also provide an independent check on the trends reported in this study.

3 ANALYSIS OF GLOBAL COLOURS

Armed with secure measurements of global and fibre colours, we now set out to find and understand any differences between the colours of paired and control galaxies.

3.1 The Dependence of Mean Colours on Δv

Our paired galaxy sample spans a line of sight rest-frame velocity difference of $0 < \Delta v < 10,000 \text{ km s}^{-1}$. Pairs with $\Delta v > 3000 \text{ km s}^{-1}$ cannot be physically close together, as the required peculiar velocities for this scenario are unphysical. We therefore will refer to these systems as *projected pairs* (interlopers), and will use them as a sanity check; specifically, we would expect any real differences

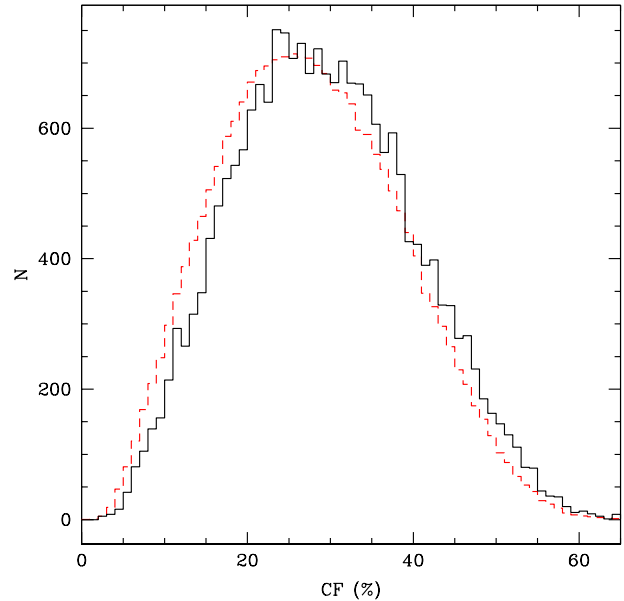


Figure 2. Histograms of r -band covering fraction (CF) are shown for paired galaxies (solid black lines) and the control sample (dashed red lines). These distributions are seen to be broadly similar, despite the fact that paired and control galaxy were not matched using covering fractions. The offset towards larger CF's for paired galaxies, which is on the order of 1.5%, is sufficiently small that it should have a negligible effect on the resulting fibre colours.

between paired and control galaxies to disappear in the projected pair sample.

In order to focus on the effects of galaxy interactions, we wish to impose a maximum Δv on our non-projected pairs sample. The primary motivation is to minimize chance superposition of non-interacting galaxies within relatively dense environments such as groups or clusters. Ellison et al. (2010) show that there is a correlation between Δv and projected galaxy density, in that pairs with higher Δv lie in regions of higher density (within their sample of pairs with $\Delta v < 500 \text{ km s}^{-1}$). To guide our choice of a maximum Δv , we plot in Figure 3 the mean global colours of galaxies in pairs as a function of Δv , considering three subsets of the pairs sample: close pairs ($r_p < 30 h_{70}^{-1} \text{ kpc}$), intermediate separation pairs ($30 < r_p < 55 h_{70}^{-1} \text{ kpc}$) and wide pairs ($55 < r_p < 80 h_{70}^{-1} \text{ kpc}$).

We find that pairs with $300 \lesssim \Delta v \lesssim 1200 \text{ km s}^{-1}$ have mean colours which are quite red with respect to both low and high velocity pairs. This is true for close, intermediate, and wide separation pairs, indicating that this trend is unlikely to be associated with galaxy interactions/mergers. Instead, we interpret these redder colours as being due to the higher densities probed by these relative velocities (Ellison et al. 2010), and the fact that galaxy colour and local density are correlated. This is consistent with the relatively high proportion of late type galaxies in low velocity pairs ($\Delta v < 200 \text{ km s}^{-1}$) reported by Park & Choi (2009). While these higher velocity pairs are certain to include some ongoing interactions and eventual mergers (and in fact clear signs of interactions are seen in the images of some systems), we elect to avoid the expected high superposition rate in this regime by imposing a maximum Δv of 200 km s^{-1} , which comfortably avoids these higher velocity environments while allowing us to retain a sizeable sample of pairs. For comparison, other

⁶ That is, for a given galaxy, the CF depends on its distance and its size; redshift and stellar mass provide a proxy for these quantities.

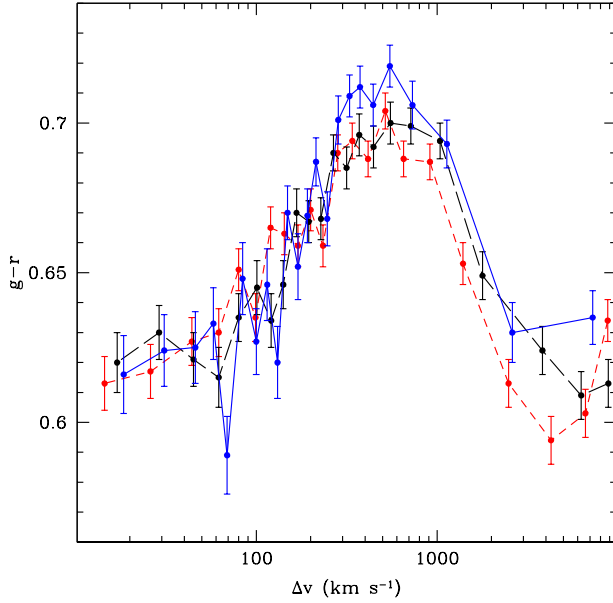


Figure 3. Mean GIM2D global colours are plotted versus rest-frame velocity difference (Δv) for three subsets of the pair sample: $r_p < 30 h_{70}^{-1}$ kpc (blue symbols; solid lines), $30 < r_p < 55 h_{70}^{-1}$ kpc (black symbols; long dashed lines), and $55 < r_p < 80 h_{70}^{-1}$ kpc (red symbols; short dashed lines). Error bars in this figure and elsewhere in the paper refer to the standard error in the mean, unless otherwise specified. Mean colours are reddest at $300 \lesssim \Delta v \lesssim 1200 \text{ km s}^{-1}$, presumably due to the fact that these pairs lie in the highest density environments.

close pair studies have imposed less restrictive Δv limits ranging from $\Delta v = 350 \text{ km s}^{-1}$ (Lambas et al. 2003; Alonso et al. 2004, 2006; Perez et al. 2009b), to 500 km s^{-1} (Patton et al. 2000, 2002; De Propris et al. 2005; Woods & Geller 2007; Ellison et al. 2008, 2010; Woods et al. 2010) and up to 1000 km s^{-1} (Barton et al. 2000; Geller et al. 2006; Barton et al. 2007).

3.2 The Dependence of Mean Colours on r_p

We now proceed to compare the colours of galaxies in low velocity pairs ($\Delta v < 200 \text{ km s}^{-1}$) with their control galaxies. In Figure 4, we plot mean global colours as a function of r_p , for both paired and control galaxies. Compared with the strong dependence of mean colour on Δv that was seen in Figure 3, we find that the global colours of low velocity pairs vary much less with r_p . The mean colour of galaxies in pairs decreases smoothly as pair separation decreases, with galaxies in the closest pairs being on average about 0.01 mag bluer than galaxies in the widest pairs. No significant change in the mean colours of the associated control galaxies is seen over this range in r_p . The closest pairs have global colours which are equivalent to their controls, whereas the widest pairs are ~ 0.01 mag redder on average.

3.3 The Distribution of $g-r$ Colours

Based on the lack of a dependence of mean colour on r_p , one might be tempted to conclude that (a) the colours of galaxies are generally unaffected by galaxy-galaxy interactions or (b) that few of the galaxies in close pairs are actually undergoing interactions. However, as has been shown elsewhere (e.g., Balogh et al. 2004), *mean*

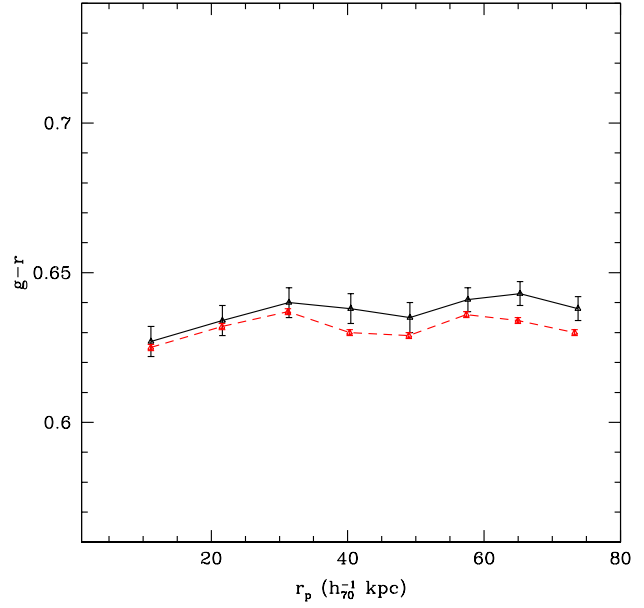


Figure 4. Mean GIM2D global colours are plotted versus projected separation (r_p) for paired galaxies (black symbols and solid line) and control galaxies (red symbols and dashed line). The sample is restricted to $\Delta v < 200 \text{ km s}^{-1}$. The vertical scale is the same as in Figure 3, thereby emphasizing that mean colours have a much stronger dependence on Δv than on r_p . The mean colours of paired galaxies decrease slightly towards small pair separations (by ~ 0.01 mag), whereas their associated control samples have mean colours that are relatively constant with respect to r_p .

colours alone are not very sensitive to changes within galaxy populations. For example, if there are excesses of both extremely red and extremely blue galaxies within samples of interacting/merging galaxies, as has been reported elsewhere (e.g., Alonso et al. 2006; Darg et al. 2010), these effects might cancel out, at least in part, when computing mean colours.

With this in mind, we now compare the colour distributions of paired and control galaxies. We begin by plotting histograms of global colours in Figure 5, for close pairs, wide pairs, and projected pairs. Overall, the distributions of paired galaxy colours are broadly similar to those of the associated controls, with a distinct red sequence and a more extended distribution of blue galaxies (the “blue cloud”). This is the aforementioned colour bimodality, within which the relative proportion of red versus blue galaxies has been found to depend on environment and luminosity (Balogh et al. 2004). However, we find a small but significant deficit in galaxies with intermediate global colours ($0.4 < g-r < 0.65$) for galaxies in close and wide pairs with $\Delta v < 200 \text{ km s}^{-1}$ (relative to their control samples), and an excess of galaxies which are relatively red (on the redward half of the red sequence peak)⁷. These differences are not seen in the projected pairs sample. In addition, a small but significant population of extremely blue galaxies ($g-r \lesssim 0.3$) is seen in the close pairs sample, but is greatly diminished in the wide pairs sample, and non-existent in the projected pairs sample. This lends support to the notion that these extremely blue galaxies may be directly associated with galaxy-galaxy interactions. We will return to this intriguing sub-population in Section 4.3.

⁷ We will revisit this excess of red galaxies in Section 4.1

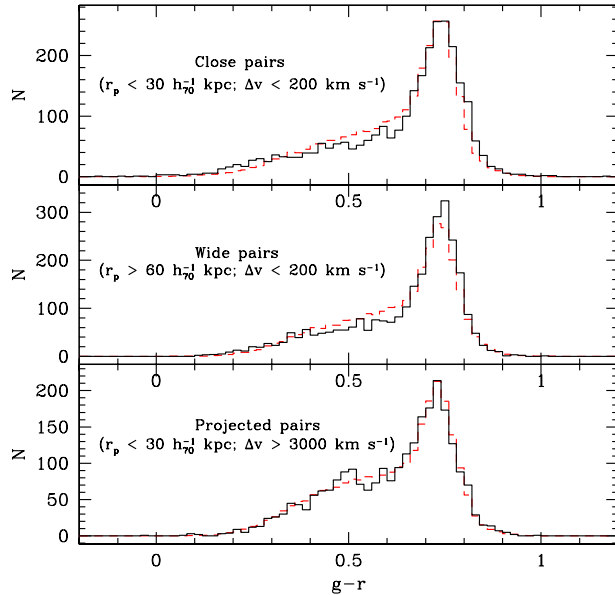


Figure 5. Histograms of global $g-r$ are shown for pairs (solid black lines) and their associated control galaxies (dashed red lines). The lower plot is for projected pairs ($r_p < 30 h_{70}^{-1}$ kpc and $3000 < \Delta v < 10,000$ km s $^{-1}$), the middle plot is for wide pairs ($r_p > 60 h_{70}^{-1}$ kpc and $\Delta v < 200$ km s $^{-1}$), and the upper plot is for close pairs ($r_p < 30 h_{70}^{-1}$ kpc and $\Delta v < 200$ km s $^{-1}$).

4 COLOUR CLASSIFICATIONS

In order to further examine these differences between paired and control sample galaxies, we now divide the sample into four subsets based on colour and absolute magnitude. Figure 6 illustrates this division of the sample into extremely red galaxies, red sequence galaxies, blue cloud galaxies, and extremely blue galaxies. The division between red sequence and blue cloud galaxies corresponds to a line with slope -0.01 which passes through $g-r = 0.65$ at $M_r = -21$. The slope provides a good fit to the colour magnitude relation seen on Figure 6, and the intercept was selected by examining the colour histograms of Figure 5. Throughout the remainder of this paper, this division is used to distinguish between red and blue galaxies.

We also identify subsets of extremely red and extremely blue galaxies. The criterion of $g-r > 0.9$ at $M_r = -21$ for extremely red galaxies applies to the reddest 1% of galaxies in projected pairs, and is sufficiently red that galaxies are unlikely to have been scattered from the red sequence (recall from § 2.4 that all galaxies are required to have $g-r$ colour errors of < 0.1 mag). This threshold is slightly less strict than the $g-r = 0.95$ cut used by Alonso et al. (2006). Our threshold for extremely blue galaxies corresponds to $g-r = 0.3$ at $M_r = -21$, and applies to the bluest $\sim 1\%$ of galaxies in the projected pairs sample. This threshold is notably stricter than the extremely blue cut of $g-r = 0.4$ employed by Alonso et al. (2006). West et al. (2009) find that rising SFRs are needed to produce colours bluer than $g-r = 0.3$.

4.1 The Red Fraction

The fraction of galaxies which are classified as red (either red sequence or extremely red), hereafter called the red fraction, is plotted versus projected separation in the lower panel of Figure 7. The red

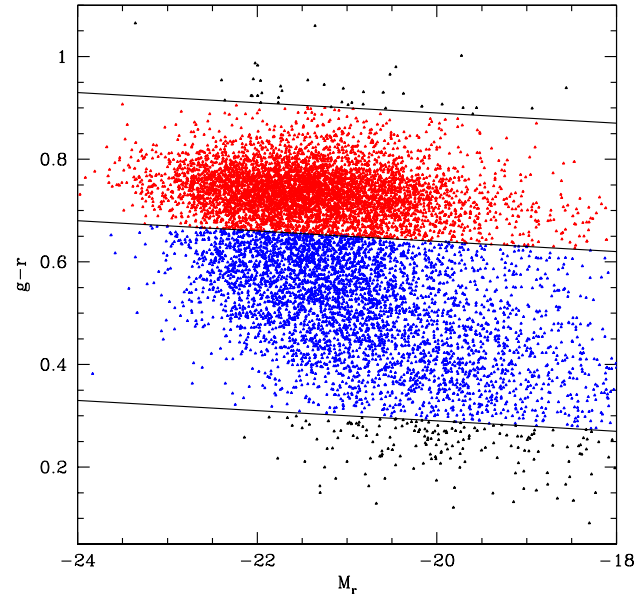


Figure 6. The colour magnitude diagram of 10000 galaxies randomly selected from the control sample is used to illustrate the division our sample into four different colour categories. The categories are: extremely red (black symbols above upper line), red sequence (red symbols), blue cloud (blue symbols), and extremely blue (black symbols below lower line). The three solid lines separate these subsets, and intersect $M_r = -21$ at $g-r = 0.9, 0.65$, and 0.3 (top to bottom). Each line has a slope of -0.01 , which provides a good fit to the observed slope of the red sequence.

fraction of paired galaxies is consistently larger than the associated control sample at all separations, although this difference may decline at smaller separations. These findings are consistent with the dependence of mean colours on separation reported in Section 3.2, and with the excess of red sequence galaxies (and corresponding deficit of blue cloud galaxies) described in Section 3.3.

We note that other studies have also reported that galaxies in pairs are significantly redder than galaxies without nearby companions (e.g., Perez et al. 2009b), with correspondingly higher bulge fractions than their isolated counterparts (Deng et al. 2008; Ellison et al. 2010). The most obvious cause of this difference would be if pairs reside in higher density environments, since the red fraction is known to increase with density (Balogh et al. 2004; Baldry et al. 2006; Cooper et al. 2006). Lin et al. (2010) show that gas-poor pairs reside preferentially in higher density environments, and that this is due primarily to the colour-density relation. Barton et al. (2007) find that paired galaxies in simulations occupy higher-mass haloes than isolated galaxies, and predict that this should lead to mean $g-r$ colours which are about 0.05 mag redder than field galaxies. The fact that we find a smaller difference than this (≤ 0.01 mag in the mean; § 3.2) is likely due to the fact that our control sample is matched to the pairs in both stellar mass and redshift, thereby providing a fairer comparison than random field galaxies.

Nevertheless, we can test this hypothesis directly by using the Baldry et al. (2006) measurements of projected local density (Σ) as a probe of environment. Σ is computed using the distances to the fourth and fifth nearest neighbours within 1000 km s $^{-1}$. These measurements have recently been updated to include DR7 galaxies. The suitability of these measurements for close pair studies is

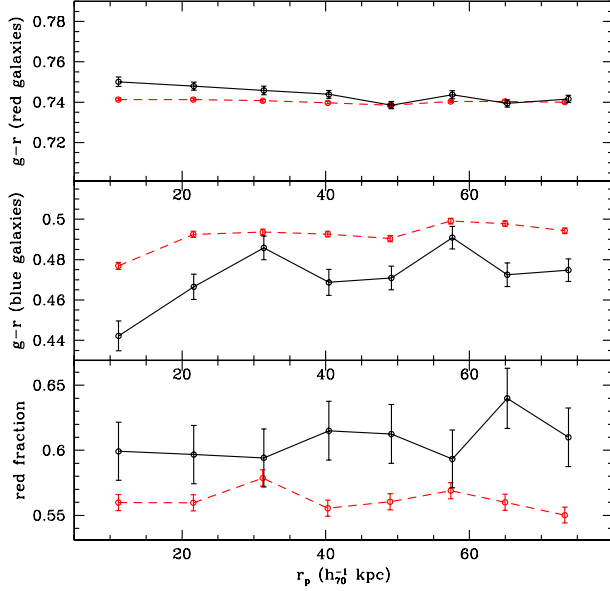


Figure 7. Trends in the global colours of blue and red galaxies with projected separation r_p are investigated. The lower plot gives the red fraction (the fraction of galaxies which are classified (see Figure 6) as red sequence or extremely red) for paired galaxies (black symbols; solid lines) and their associated control galaxies (red symbols; dashed lines). The middle plot gives the mean colour of blue galaxies (those classified as blue cloud or extremely blue), and the upper plot gives the mean colour of red galaxies (those classified as red sequence or extremely red).

addressed by Ellison et al. (2009, 2010). The Baldry et al. (2006) requirement for redshifts to lie within the range 0.010–0.085 means that these measurements are available for only 57% of the galaxies in our full pairs sample. However, as our control sample is matched in redshift to the pair sample, we are still able to make a fair comparison between the local densities of paired and control galaxies.

In Figure 8, we provide histograms of Σ for paired and control galaxies. As with Figure 5, we separate our pairs sample into close pairs, wide pairs, and projected pairs. We find that galaxies in close and wide pairs are skewed to higher local densities than their associated control galaxies, with this difference being nearly two times larger in wide pairs than in close pairs. No significant difference is seen in the Σ distributions of projected pairs and their control galaxies. These findings are consistent with the hypothesis that the higher fraction of red galaxies in close and wide pairs is due to these systems residing in higher density environments than their control galaxies, and the inference that more of these pairs result from chance superpositions in overdense regions (Alonso et al. 2004; Perez et al. 2006). Moreover, the fact that this excess is more pronounced for wide pairs than close pairs is consistent with the expectation that chance superpositions within groups and clusters should be more common in wide pairs than in close pairs (Alonso et al. 2004; Lin et al. 2010).

4.2 The Colours of Red and Blue Galaxies

We now proceed to assess the colours of red and blue galaxies separately. The middle and upper panels of Figure 7 show the mean colours of galaxies classified as blue (blue cloud or extremely blue) and red (red sequence or extremely red) respectively. In both cases

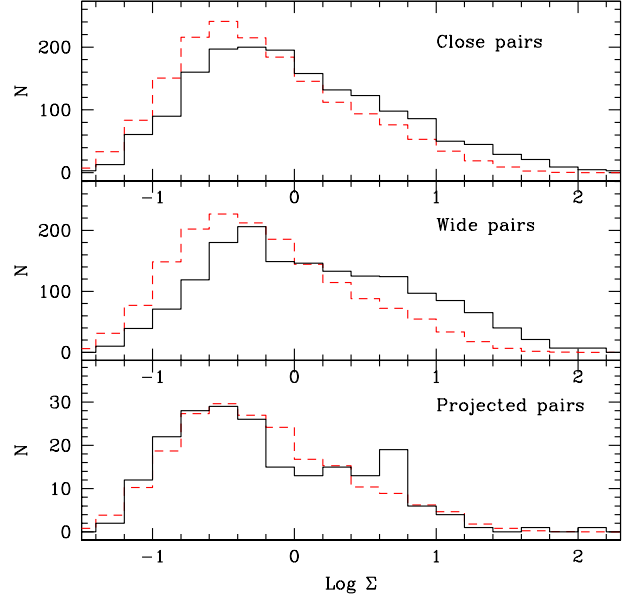


Figure 8. Histograms of projected local density Σ are shown for pairs (solid black lines) and their associated control galaxies (dashed red lines). The lower plot is for projected pairs ($r_p < 30 h_{70}^{-1}$ kpc and $3000 < \Delta v < 10,000$ km s $^{-1}$), the middle plot is for wide pairs ($r_p > 60 h_{70}^{-1}$ kpc and $\Delta v < 200$ km s $^{-1}$), and the upper plot is for close pairs ($r_p < 30 h_{70}^{-1}$ kpc and $\Delta v < 200$ km s $^{-1}$).

we see clear differences between paired and control galaxies. Blue galaxies in pairs are bluer than blue galaxies in the control sample at all separations, with a typical offset decreasing from ~ 0.03 mag for close pairs ($r_p < 30 h_{70}^{-1}$ kpc) to 0.02 mag for wide pairs ($r_p > 60 h_{70}^{-1}$ kpc). In contrast, red galaxies in pairs are *redder* than red control galaxies by ~ 0.01 mag at the closest separations, with this relatively small offset becoming negligible beyond $\sim 25 h_{70}^{-1}$ kpc. The fact that these trends go in opposite directions (bluward and redward) means that they will reduce any associated trends in mean colour or red fraction, which is consistent with our findings in Sections 3.2 and 4.1.

4.3 Extremely Blue and Extremely Red Galaxies

In Section 3.3 and Figure 5, we noted a population of extremely blue galaxies which are present in the close pair sample but nearly absent in the wide pair sample (and non-existent in the projected pair sample). This is reminiscent of the excess populations of extremely blue galaxies reported in several close pair studies (Alonso et al. 2006; Perez et al. 2009b; Darg et al. 2010), although we do not detect an obvious population of extremely red galaxies as found in these same studies.

To explore this further, we first plot the fraction of galaxies in our $\Delta v < 200$ km s $^{-1}$ pairs which are extremely blue in the lower left panel of Figure 9. We find a clear excess of extremely blue galaxies, rising from $\sim 3\%$ at wide separations to $\sim 7\%$ at small separations. A similar but less pronounced trend is seen in the control sample, implying that part of the trend in paired galaxies is due to a change in the mix of stellar mass and/or redshift with separation. We repeat these measurements for our sample of projected pairs ($3000 < \Delta v < 10,000$ km s $^{-1}$) in the middle left panel

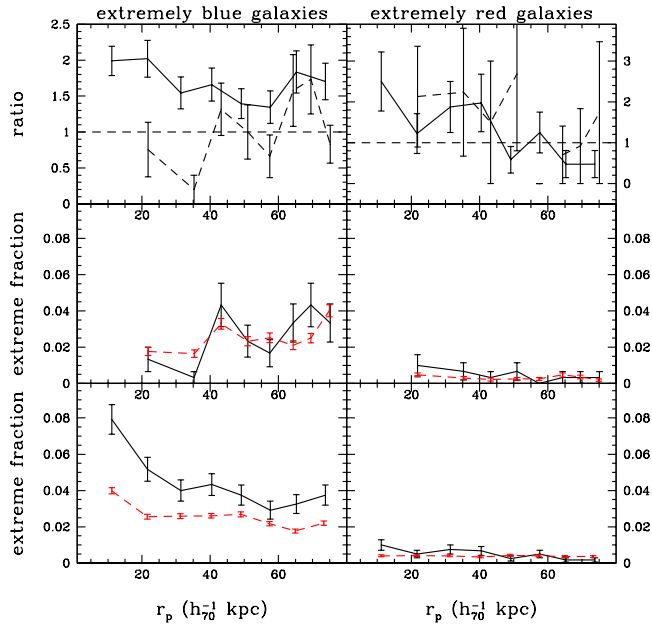


Figure 9. The prevalence of extremely blue (red) galaxies is explored using three plots in the lefthand (righthand) column. The lower panels report the fraction of galaxies which are extremely blue or red for low velocity ($\Delta v < 200 \text{ km s}^{-1}$) pairs, whereas the middle panels refer to projected pairs ($3000 < \Delta v < 10,000 \text{ km s}^{-1}$). In the lower and middle plots, black symbols and solid lines refer to paired galaxies, while red symbols and dashed lines refer to control galaxies. The upper panels report the ratio of extremely blue/red fractions for pairs vs. control for low velocity pairs (solid black lines) and projected pairs (dashed black lines). The black horizontal dashed line in the upper panel corresponds to a ratio of one (i.e., no difference between pairs and control). All error bars in this plot refer to Poisson errors.

of Figure 9, finding no rise as r_p decreases⁸. This essentially rules out the possibility that the rise towards small r_p seen for true close pairs could be due to poor photometry in crowded pairs. Finally, we also compute the ratio of the extremely blue fractions in pairs versus control (upper left hand panel of Figure 9), in order to see how the rise in the extremely blue fraction of pairs compares with the rise for the control sample. Contrary to what is observed for projected pairs (dashed line), the ratio for low velocity pairs (solid line) is significantly higher than unity throughout the full range of r_p , rising from about 1.5x for wide pairs to about 2x for the closest pairs.

In the right hand panels of Figure 9, we apply the same approach to the extremely red galaxies. We find a much lower fraction of galaxies in this category, rising from $\sim 0.3\%$ for wide pairs to $\sim 1\%$ for the closest pairs. The control sample remains constant at about 0.4% for all separations. The ratio of pairs to control exhibits a gradual rise in extremely red galaxies towards the smallest pair separations, reaching a factor of 2.5x at $r_p \sim 10 h_{70}^{-1} \text{ kpc}$. However, a comparable rise is also seen in the projected pairs sample, leading

us to believe that this rise may be due to residual problems with the photometry of crowded systems.

Together, our results are qualitatively consistent with the high fractions of extremely blue galaxies in pairs reported by Alonso et al. (2006), Perez et al. (2009b), and Darg et al. (2010), but appear to be at odds with the substantial fractions of extremely red galaxies described in these same studies. For example, Alonso et al. (2006) find extremely red fractions ranging from ~ 7 to 16% for three different environmental classes, using a *stricter* criterion ($g - r > 0.95$) than we do ($g - r > 0.9$ at $M_r = -21$).

4.4 The Impact of Photometric Quality on Extremely Red/Blue Galaxies

We have found that a substantial number of galaxies in pairs are classified as extremely blue (up to $\sim 7\%$ in the closest pairs), whereas very few are classified as extremely red ($\leq 1\%$ in the closest pairs). The widest pairs also contain roughly 50% more extremely blue galaxies than the control sample, but no excess of extremely red galaxies. Moreover, the trends seen in the extremely blue (red) fraction are absent (present) in the projected pairs sample. This implies that poor photometry cannot explain the extremely blue population, but may explain the extremely red population.

Simard et al. (2010) provide a clear demonstration that the standard SDSS pipeline does a poor job of galaxy photometry for closely separated pairs, whereas their recomputed GIM2D global colours are much more secure. To directly assess the effects of using these different measurements of $g - r$ colours, we compute the extremely blue and extremely red fractions in Figure 10, using our GIM2D global colours (bottom row), SDSS Petrosian colours (middle row), and SDSS modelMag colours (top row). Exactly the same set of paired and control galaxies is used in each case. The rise in the extremely blue fraction of close pairs towards small separations is seen with all three colour indices. Conversely, a large increase in the extremely red fraction of close pairs towards small separations is seen only with SDSS Petrosian and modelMag colours, reaching 6% and 8% respectively.

This provides compelling evidence that poor photometry is in fact largely responsible for the large extremely red fractions seen in close pairs when using photometry directly from SDSS, and that the re-computed colours used in our analysis are effective in removing nearly all of these anomalously red systems. Related factors which may contribute to the lower extremely red fractions found in our study include our imposition of a bright apparent magnitude limit of $m_r > 14.5$ (which allows us to avoid the brightest galaxies where deblending is particularly problematic) and our use of a lower relative velocity threshold than most other studies (which preferentially avoids pairs in more crowded regions).

We caution that the small rise in our GIM2D extremely red fraction at small r_p could be due to residual effects from poor photometry in crowded systems. More importantly, it seems likely that published reports of large fractions of extremely red galaxies in close pairs or merging galaxies (e.g., Alonso et al. 2006; Perez et al. 2009b; Darg et al. 2010) are the result of poor SDSS photometry, rather than dust obscuration or other physical effects associated with induced star formation.

Further insight into the nature of these extremely blue and extremely red galaxies can be gleaned by visual inspection of their images, as shown in Figure 11. Clear morphological signs of interactions are seen within both sets of galaxies. There are obvious indications of dust in some of the extremely red galaxies. Some of this dust could have been stirred up as a result of galaxy interactions

⁸ We note that there are far fewer projected pairs ($3,000 < \Delta v < 10,000 \text{ km s}^{-1}$) than low velocity pairs ($\Delta v < 200 \text{ km s}^{-1}$), since correlated pairs are much more common than chance superpositions. This explains why the error bars on the projected pairs sample are larger, and why these data do not extend as far inwards in r_p .

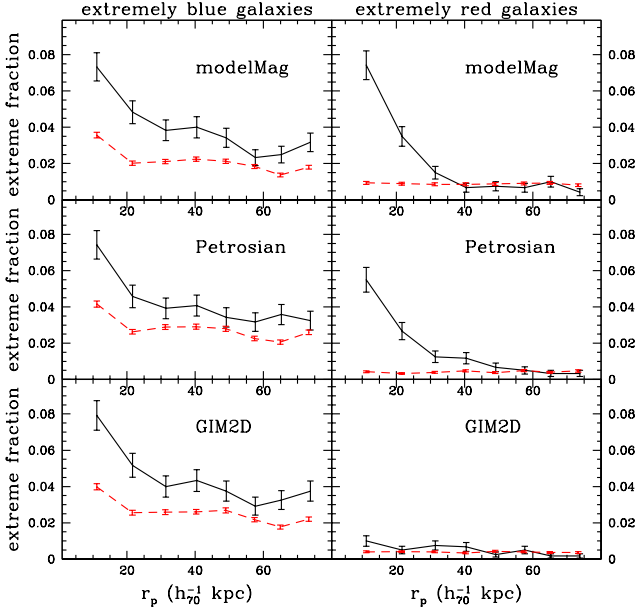


Figure 10. The fraction of extremely blue (red) galaxies is plotted in the lefthand (righthand) column for three different indices of $g-r$ colours. The lower plots reports the global GIM2D colours used in our analysis. The middle and top panels instead employ SDSS-measured Petrosian and modelMag colours respectively, for the same galaxies. Pairs are displayed using black symbols and solid lines, while the associated control galaxies are displayed using red symbols and dashed lines. All error bars in this plot refer to Poisson errors.

(e.g., Geller et al. 2006). However, in some cases, the dust is associated with edge-on discs; the ensuing reddening might be expected to be on the order of 0.1 mag in $g-r$ (Masters et al. 2010). Nevertheless, edge-on discs would be expected to be present in equal measure in the control sample, so they are unlikely to be responsible for differences between paired and control galaxies.

Finally, we note that these images provide vivid evidence of the well-known Holmberg effect (Holmberg 1958), in that galaxies within individual pairs tend to have colours which are similar to one another (i.e., there are few red-blue pairs).

5 FIBRE COLOURS

In Section 2.5, we described our computation of rest-frame fibre colours, and the suitability of these colours as a probe of central (rather than global) star formation. In this section, we begin by analyzing the distribution of fibre colours in close, wide and projected pairs. We then investigate the differences between fibre and global colours.

5.1 The Distribution of Fibre Colours

In Figure 12, we compare the fibre colours of paired and control galaxies, for close, wide and projected pairs. We find a small but significant excess of extremely blue galaxies in close pairs, which is barely detectable in wide pairs and absent in projected pairs. On the other hand, we find no excess of paired galaxies with extremely red fibre colours. This is consistent with our hypothesis in § 4.4 that residual problems with the photometry of crowded systems is

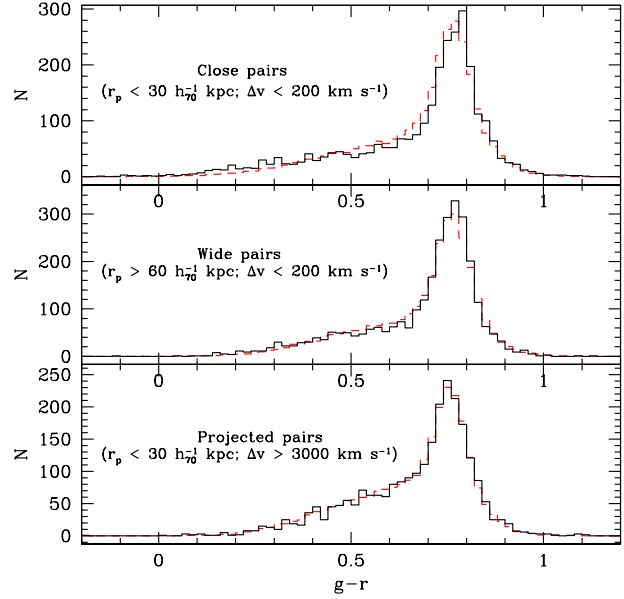


Figure 12. Histograms of fibre $g-r$ are shown for pairs (solid black lines) and their associated control galaxies (dashed red lines). The lower plot is for projected pairs ($r_p < 30 h_{70}^{-1}$ kpc and $3000 < \Delta v < 10,000$ km s $^{-1}$), the middle plot is for wide pairs ($r_p > 60 h_{70}^{-1}$ kpc and $\Delta v < 200$ km s $^{-1}$), and the upper plot is for close pairs ($r_p < 30 h_{70}^{-1}$ kpc and $\Delta v < 200$ km s $^{-1}$).

responsible for the small population of galaxies with extremely red global colours, since this effect should be much smaller when using fibre colours.

We also find a significant deficit of galaxies in close pairs with intermediate fibre colours ($0.5 < g-r < 0.75$), and a corresponding excess of galaxies on the red half of the red sequence. This effect is smaller than was seen using global colours, particularly for wide pairs. We again attribute this difference between paired and control galaxies to the higher density environments of paired galaxies.

5.2 The Difference Between Fibre and Global Colours

In the preceding subsection, we compared the distributions of fibre colours in close, wide and projected pairs to those found using global colours. While useful, this approach does not tell us how fibre and global colours compare on a galaxy-by-galaxy basis. If a subset of interacting galaxies experience centrally-concentrated bursts of star formation, we might expect to find evidence of this effect in the colour gradients of these galaxies. In this section, we will use the difference between fibre and global colour as a probe of this effect.

In Figure 13, we plot the difference between fibre and global colour versus global colour for four subsets of the pairs sample: close low velocity pairs (upper left panel), wide low velocity pairs (lower left panel), close projected pairs (upper right panel), and wide projected pairs (lower right panel). Overall, fibre colours are redder than global colours; i.e., $g-r$ (fibre) - $g-r$ (global) is positive. This is as expected, given that bulges are generally redder than discs. The difference between fibre and global colours is largest for galaxies of intermediate colour. The most obvious explanation is that galaxies of intermediate colour are the least likely to be either bulge-dominated or disc-dominated galaxies. In any case, we are

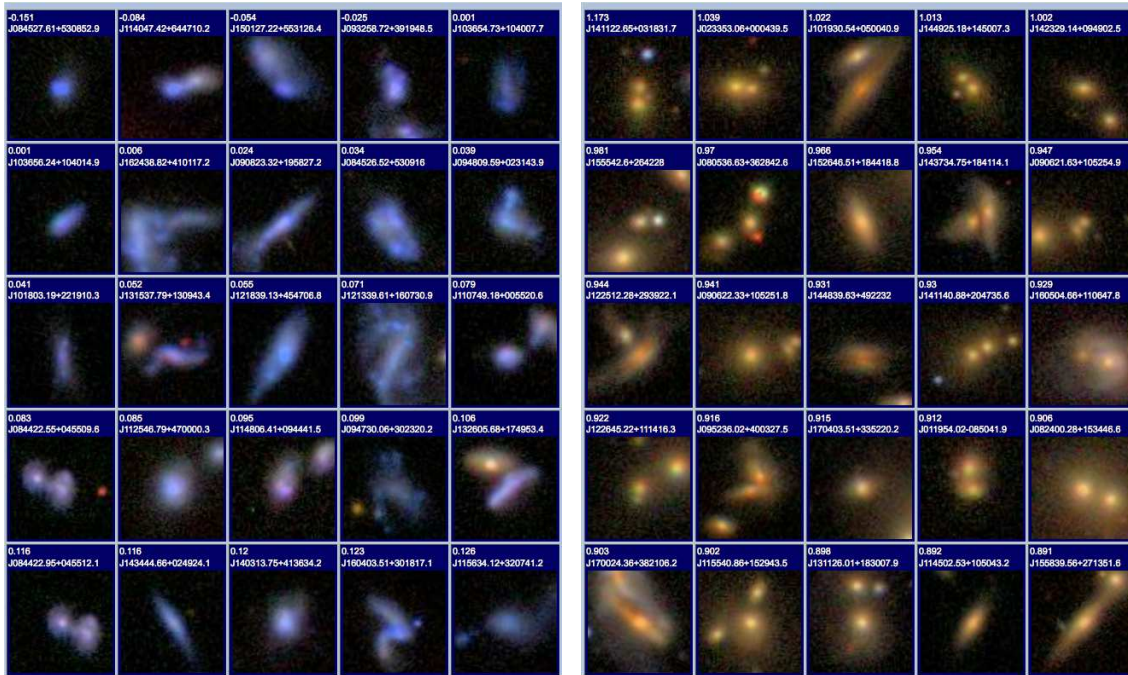


Figure 11. Images of galaxies in close pairs ($r_p < 30 h_{70}^{-1}$ kpc and $\Delta v < 200$ km s $^{-1}$) which have the bluest (left panel) and reddest (right panel) global colours. The colours are labelled in the top left of each image, and galaxies are sorted according to colour within each panel, with the most extreme at the upper left.

primarily interested in how this index differs between paired and control galaxies.

Figure 13 shows that, for red galaxies, there is good agreement between the fibre-global colours of paired and control galaxies, for both wide and close pairs. Conversely, for blue galaxies, close low velocity pairs have fibre colours which are typically 0.03 mag bluer than those of their associated control galaxies (upper left panel), with this difference dropping to 0.015 mag for wide low velocity pairs (lower left panel). This difference is absent in the projected pairs sample (right hand panels), confirming that crowding cannot be responsible for the offset. This is a highly significant effect, and is our strongest indication yet that centrally triggered star formation is taking place in some of these systems. Figure 14 gives a particularly striking example of a system in which morphological signs of an interaction accompany a relatively blue central colour. The fact that the mean offset is largest in close pairs, but still present in wide pairs, implies that the effects of this star formation on galaxy colours diminishes as galaxies move apart after close encounters, but that the effects persist long enough that they are still present in some widely separated pairs. We explore this scenario further in Section 7.

6 COLOUR OFFSETS

The increase in extremely blue galaxies in close pairs, combined with the relatively high *red* fraction of galaxies in close and wide pairs, demonstrates that galaxies in pairs can be either bluer or redder than their control counterparts, for different reasons. The former appears to be caused by ongoing galaxy-galaxy interactions, whereas the latter can be attributed to the higher density environment occupied by paired galaxies, and may therefore be true for pre-interaction galaxy pairs too.

In principle, these competing effects mean that some of the

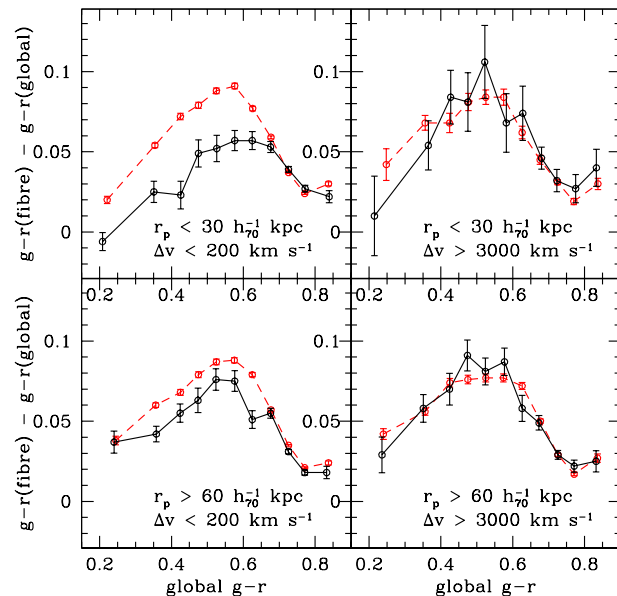


Figure 13. The difference between fibre and global colours is plotted versus global colour for four subsets of the pairs sample: close low velocity pairs (upper left panel), wide low velocity pairs (lower left panel), close projected pairs (upper right panel), and wide projected pairs (lower right panel). Paired galaxies are shown with black symbols and solid lines, while the associated control galaxies are shown with red symbols and dashed lines. Larger values of this colour difference correspond to redder centres.

colour differences between paired and control galaxies will cancel out when comparing their colour distributions. That is, only the *net changes* in the colour distributions will be detected. However,



Figure 14. An SDSS *gri* image of a close galaxy pair which exhibits clear signs of a blue nucleus that may have been triggered by an interaction. The galaxy on the left (objID=587731513153159199) has a fibre colour which is 0.22 mag bluer than its global colour. This pair has a projected separation of $26 h_{70}^{-1}$ kpc and $\Delta v = 109 \text{ km s}^{-1}$.

it may be possible to uncover more of the underlying colour differences by comparing, *on an individual basis*, the colour of every paired galaxy with the ~ 12 galaxies in its associated control sample. This method has the potential to detect much more of the underlying differences in galaxy colours, and may even allow us to identify which galaxies have had their colours changed the most as a result of ongoing/recent interactions.

To this end, we compute the *colour offset* for every paired galaxy in the sample. We define colour offset as the colour of the paired galaxy minus the mean colour of its associated (~ 12) control galaxies. We also compute the colour offset of every control galaxy, by computing the difference between its colour and the mean colour of the remaining ~ 11 associated control galaxies. We then compute the difference between the colour offsets of paired and control galaxies (hereafter, we will refer to this quantity as $\Delta(g-r)$). If paired galaxy colours are drawn at random from the same parent population as control galaxies, we would expect to find $\Delta(g-r)$ to be zero, on average.

Figure 15 plots $\Delta(g-r)$ as a function of projected separation for low and high velocity pairs, and treats blue and red galaxies separately. The left hand column of this figure refers to global colours, while the right hand column refers to fibre colours. For blue galaxies, a highly significant negative (blueward) fibre colour offset is found in low velocity pairs, changing smoothly from about 0.02 mag for wide pairs to about 0.075 mag for the closest pairs. At the smallest separations, this difference is significant at the 11σ level. This trend is much more modest in global colours, reaching ~ 0.02 mag for the closest pairs. This trend is absent in the high velocity (projected) pair sample, demonstrating that crowding errors cannot be responsible for this effect.

Images of blue galaxies in very close pairs ($r_p < 15 h_{70}^{-1}$ kpc) which have the greatest blueward offsets are presented in Figure 16. Many of these systems exhibit clear morphological signs of interactions, along with indications of relatively blue central colours. This demonstrates that our colour offset parameter does in fact appear to be effective at identifying systems with atypical star forming prop-

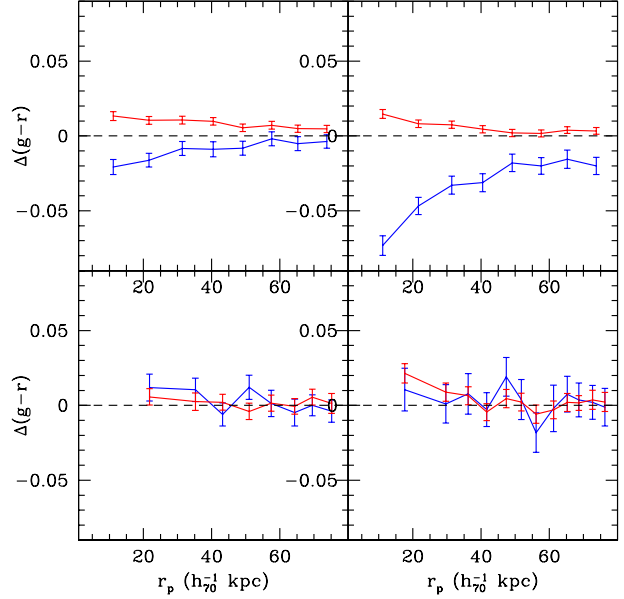


Figure 15. The difference between the offset of paired and control galaxies ($\Delta(g-r)$) is plotted versus r_p for low velocity pairs ($\Delta v < 200 \text{ km s}^{-1}$; upper panels) and high velocity pairs ($\Delta v > 3000 \text{ km s}^{-1}$; lower panels). The left hand panels refer to global colours, while the right hand panels refer to fibre colours. Blue symbols refer to blue galaxies (those with global $g-r \leq 0.65$ for $M_r = -21$), and red symbols refer to red galaxies ($g-r > 0.65$ for $M_r = -21$). In all plots, the dashed horizontal line at $\Delta(g-r) = 0$ denotes the null hypothesis of no colour changes in paired galaxies.

erties (note that more than half of the galaxies in Figure 16 do not qualify as extremely blue, and therefore do not stand out when using colour rather than colour offset). Together, these results are consistent with the presence of central induced star formation which is strongest in the closest pairs and weaker (but still present) in wide pairs.

A much weaker trend is found for red galaxies in low velocity pairs, with an increase (reddening) in $\Delta(g-r)$ of up to 0.015 mag for the closest pair separations. The size of this effect is the same in fibre and global colours, implying that the effect is global. However, it appears from Figure 15 that a comparable trend may also be present in the projected pairs sample; therefore, we are unable to rule out the possibility that crowding errors are responsible for this trend.

6.1 Dependence on Projected Local Density

In a related study, Ellison et al. (2010) found a small bluing of the bulges, and not the discs, of galaxies in close low velocity pairs. This effect was seen only at low densities, and was interpreted as evidence of central triggered star formation. Given the striking blueward fibre offsets seen in the upper right panel of Figure 15, we now investigate the dependence of this effect on projected local density (Σ). Measurements of Σ are available for 57% of our paired galaxies, as described in Section 4.1. We subdivide our sample into three equal bins (tertiles) of Σ , and present the global and fibre colour offsets of each in Figure 17.

This figure indicates clearly that the blueward fibre offsets at small separations are driven by blue galaxies residing in low and medium density environments, though a small blueward fibre offset



Figure 16. Images of blue galaxies ($g - r < 0.65$ for $M_r = -21$) in very close pairs ($r_p < 15 h_{70}^{-1}$ kpc and $\Delta v < 200 \text{ km s}^{-1}$) are shown for galaxies which have the greatest blueward offsets in fibre colours. The offsets are labelled in the top left of each image, and galaxies are sorted according to offset (greatest offset at the upper left).

is also detected in the highest density tertile. Small blueward offsets in *global* colours (left hand column of Figure 17) are seen at small separations at low and medium densities, but not at high density. The fact that the total (blue+red) population closely traces the red population in the high density regime and traces the blue population in the low density regime is consistent with the well known colour-density relation, whereby the red fraction increases with density (see § 4.1).

Compared with figure 9 of Ellison et al. (2010), we find a larger and more significant difference between the colours of paired and control galaxies at small separations, and we find that this difference extends further into the medium- to high-density regime. We attribute this added sensitivity to triggered star formation to several factors: (1) our DR7 pairs sample is larger than the DR4 sample of Ellison et al. (2010), (2) we have approximately 3 times as many control galaxies per paired galaxy as Ellison et al. (2010), (3) colour offsets are sensitive to colour differences on a galaxy-by-galaxy basis, and (4) treating blue and red galaxies separately is effective in isolating the effects of triggered star formation to the (blue) population of galaxies which is most susceptible to this process.

6.2 The Effects of Matching Control Galaxies on Density

One significant difference between our study and several other close pair studies (e.g., Alonso et al. 2006; Perez et al. 2009b; Ellison et al. 2010) is that we do not attempt to match our control sample to the projected local densities of paired galaxies. As

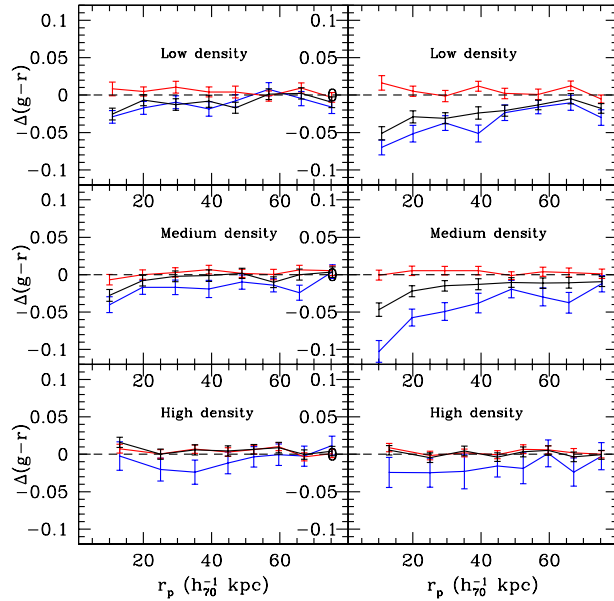


Figure 17. The difference between the offset of paired and control galaxies ($\Delta(g - r)$) is plotted versus r_p for low velocity pairs ($\Delta v < 200 \text{ km s}^{-1}$) for three tertiles in projected local density: low density (upper panels), medium density (middle panels), and high density (lower panels). The left hand panels refer to global colours, while the right hand panels refer to fibre colours. Blue symbols refer to blue galaxies (those with global $g - r \leq 0.65$ for $M_r = -21$), red symbols refer to red galaxies ($g - r > 0.65$ for $M_r = -21$), and black symbols refer to all galaxies (i.e., blue and red). In all plots, the dashed horizontal line at $\Delta(g - r) = 0$ denotes the null hypothesis of no colour changes in paired galaxies.

demonstrated in Section 4.1, our resulting control sample is skewed to lower densities than the pairs sample. This has some implications for the interpretation of differences between paired and control galaxies in our study.

We therefore investigate this issue by regenerating Figure 15 using a control sample which is matched on local density. This revised control sample is generated using the same methodology as outlined in Section 2.3, but now matching simultaneously on redshift, stellar mass and Σ . However, since it is more difficult to find matches for paired galaxies in the highest density environments, we restrict our analysis to galaxies with $\log(\Sigma) < 1.25$ (this excludes 12% of galaxies in our paired sample). We are able to find 3 control galaxies per paired galaxy.

The results are given in Figure 18. Comparison with Figure 15 reveals very similar trends in colours offsets. With a density-matched control sample, there is a slight blueward shift in the global and fibre colour offsets of blue and red galaxies. This small shift may result from the removal of galaxies in the highest density regime, since we know from Figure 17 that galaxies in the highest density environments exhibit the smallest blueward colour offsets. Another factor which may contribute to this shift is the fact that our revised control sample is no longer biased towards lower densities than paired galaxies; this would be expected to further accentuate the blueward colour offsets in pairs due to induced star formation. We conclude that the main results of our study are unchanged if a density-matched control sample is used.

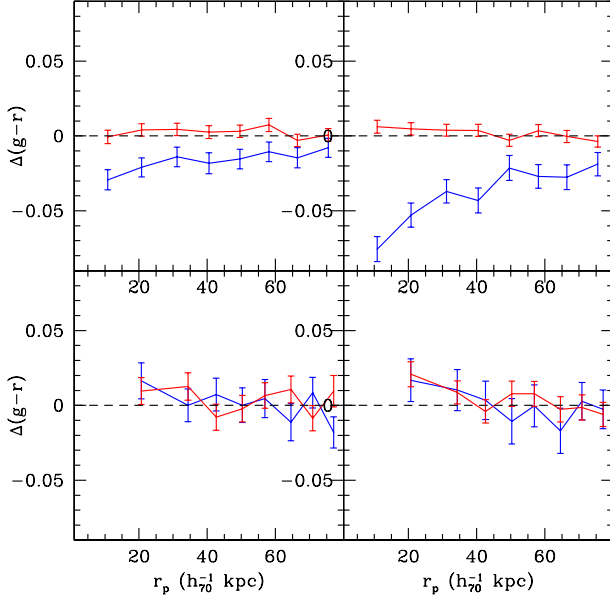


Figure 18. This figure presents the same information as Figure 15, but restricts the analysis to galaxies with $\log(\Sigma) < 1.25$ and uses a control sample which is matched on redshift, stellar mass and projected local density.

7 A SIMPLE STARBURST MODEL

The interpretation of the colours of interacting galaxies can be aided by employing model starbursts which predict how colours evolve during and after a starburst. We create a simplistic galaxy+starburst model by starting with two pre-existing galaxies (a red sequence galaxy and a blue cloud galaxy) and superimposing a model starburst upon each. The goal here is to see how the colour of each galaxy changes with time as a result of the superimposed starburst. For the colours of the starburst itself, we use an instantaneous Starburst99 model starburst (Leitherer et al. 1999), with $Z = 0.020$, $\alpha = 3.30$, and $M_{\text{up}} = 100M_{\odot}$, converting from model $V - R$ colours to SDSS $g - r$.⁹ We monitor these colours for 1 Gyr following the starburst. For the pre-existing blue cloud galaxy, we use a Starburst99 model galaxy with a continuous star formation rate of $5M_{\odot}/\text{year}$, and add the instantaneous starburst after 10 Gyr. This galaxy has a $g - r$ colour of 0.43 immediately preceding the starburst, and is therefore representative of the blue cloud galaxies seen in Figure 6. For the pre-existing red sequence galaxy, we begin with an instantaneous starburst, and let it age for 10 Gyr, yielding a galaxy colour of 0.83, which lies within the red tail of the red sequence seen in Figure 6. We then add the model starburst and monitor how the galaxy’s colour changes.

The evolution in colours of these galaxy+starburst models is shown in Figure 19, for burst strengths (by stellar mass) of 10%, 20%, and 30%. This figure shows that a 20% starburst within a pre-existing red sequence galaxy will cause the galaxy to become bluer by ~ 0.15 mag, with this offset persisting for ~ 400 Myr before gradual reddening begins. Even at 1 Gyr after the starburst, this galaxy is considerably bluer than it was initially. Conversely, for a starburst that occurs in a blue cloud galaxy, the galaxy will

become ~ 0.05 mag bluer for about 400 Myr, and will return to its pre-starburst colour after 1 Gyr.

To compare with our results from the previous section, we note that the difference in colour offset between paired and control galaxies (see Figure 15) should be analogous to the offsets between our model starburst galaxies and their pre-existing counterparts (Figure 19), if all galaxies in our close pair sample were undergoing interactions with induced star formation. In reality, of course, not all of the galaxies in close pairs can be undergoing interactions, as some will not be close in three dimensions (i.e., interlopers), some will be approaching one another and therefore will not yet have had a close encounter, and others may be undergoing interactions without triggered star formation. Therefore, we would expect the mean colour offsets in our close pairs sample to be smaller than our model predictions, perhaps by a factor of a few.

In Figure 15, we found that blue galaxies in close pairs have mean global colour offsets which are ~ 0.02 mag bluer than their control galaxies. This is smaller than the ~ 0.05 mag offset predicted for a 20% starburst in a blue galaxy (Figure 19), but consistent within the hypothesis that 40% of galaxies in close pairs are experiencing induced starbursts of this strength. We find a much higher offset of 0.075 mag in fibre (rather than global) colours. This makes sense if the fractional starbursts in the central regions of these galaxies are substantially higher than 20%, as would be the case if most of the induced star formation is centrally concentrated, as implied by Figure 13. Finally, the blueward offsets we detect decrease markedly going from close to wide pairs. This is consistent with the aging and subsequent reddening of our models in Figure 19, and implies that we are seeing starbursts age as galaxies in close pairs separate following close peri-centre encounters. The fact that this offset is still visible at the largest separations probed ($80 h_{70}^{-1}$ kpc) is consistent with a simple calculation showing that a pair of galaxies separating at 200 km s^{-1} in the plane of the sky will take ~ 400 Myr to reach $r_p \sim 80 h_{70}^{-1}$ kpc.

For red galaxies, we find a small *redward* offset in close pairs (Figure 15), which may be due to residual errors with the photometry. We see no indications of the potentially large blue colour offsets that are predicted by our model galaxy+starburst for red galaxies. This appears to indicate that starbursts of order 10-30% are not commonly found in red galaxies. While it is obvious that sufficiently large offsets would move red sequence galaxies into the blue cloud, the absence of even a small blueward offset for typical red galaxies appears to rule out this scenario. This finding is not unexpected, however, given that red sequence galaxies are generally depleted in gas, and therefore less capable of triggered star formation. While deep imaging reveals that gas-poor (early type) galaxies show frequent signs of tidal disturbances, these signs of interactions are not generally accompanied by star formation (Tal et al. 2009; Ellison et al. 2010; Kaviraj 2010). Woods & Geller (2007) find a correlation between the specific SFR and pair separation for galaxies in blue pairs, but not in red pairs, confirming this interpretation. Moreover, while few red mergers contain significant amounts of dust (Whitaker & van Dokkum 2008), Gallazzi et al. (2009) find that, in intermediate to high density environments (within which many of our close pairs lie), galaxies which have had most of their star formation suppressed tend to have their remaining star formation obscured. In summary, it appears that red sequence galaxies in close pairs exhibit little in terms of induced star formation in the optical, with few (if any) unobscured starbursts with large burst strengths.

⁹ We use the Lupton (2005) colour transformations found at <http://www.sdss.org/dr5/algorithms/sdssUBVRITransform.html>.

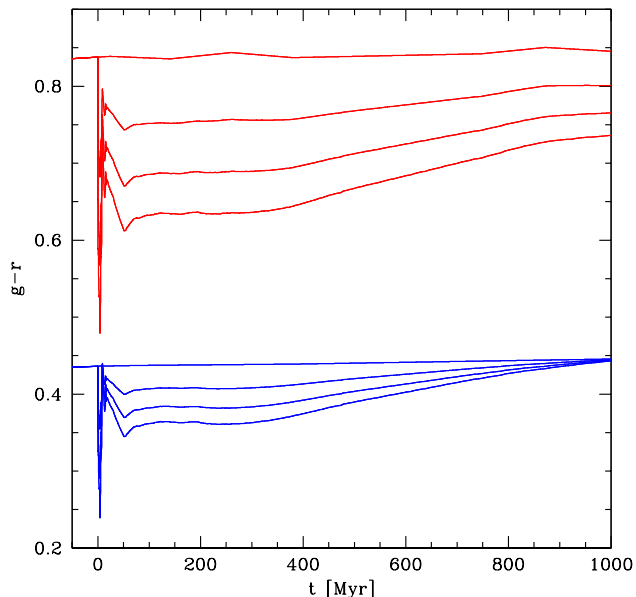


Figure 19. The colour evolution due to starbursts is modelled by adding Starburst99 model starbursts to a pre-existing red sequence and blue cloud galaxy. The uppermost red (blue) line shows the colour evolution of the red sequence (blue cloud) galaxy without a starburst. After adding starbursts at time $t=0$ with burst strengths (by stellar mass) of 10%, 20%, and 30% (top to bottom), the colour evolution of the resulting galaxies is followed for 1 Gyr. Both galaxies become bluer initially, followed by a gradual reddening. The colour change is about three times larger for the red sequence galaxy, due to the fact that the starburst is much bluer than the pre-starburst galaxy. After 1 Gyr, the late-type galaxy has returned to its pre-burst colour, whereas the early-type galaxy is still noticeably bluer.

8 CONCLUSIONS

We have compiled a large, well-defined sample of 21,347 SDSS DR7 galaxies in pairs with $r_p < 80 h_{70}^{-1}$ kpc, $\Delta v < 10,000$ km s $^{-1}$, and stellar mass ratios between 0.1 and 10. We have measured high quality $g-r$ global colours for each galaxy, and have acquired their central (fibre) colours. We have also created a very large control sample which is matched to the pairs sample in stellar mass and redshift, with ~ 12 control galaxies associated with every paired galaxy. By comparing galaxies in close pairs with their control samples, with wider separation pairs, and with close projected pairs (i.e., interlopers), we have been able to distinguish trends which are associated with interactions from those which are due to differences in environment or those which result from photometric errors due to crowding. Our findings can be summarized as follows:

(i) 60% of galaxies in close and wide pairs are classified as red, compared with 56% of control galaxies. These paired galaxies are found in higher density environments than their controls. We interpret these results as an indication that galaxies which are involved in interactions are preferentially red before the interactions start, due to the older stellar populations which are present in higher density environments.

(ii) Galaxy-galaxy interactions make blue galaxies in close pairs ($r_p < 30 h_{70}^{-1}$ kpc and $\Delta v < 200$ km s $^{-1}$) bluer by an average of 0.075 mag in fibre colours, and 0.02 mag in global colours. These colour offsets are diminished but still detectable out to pair separa-

tions of at least $80 h_{70}^{-1}$ kpc, and are strongest at low and medium projected local densities.

(iii) The fraction of extremely blue galaxies rises from about 3% for wide pairs to 8% for close pairs. The use of projected pairs (interlopers) and alternate colour measurements confirm that this effect is not due to photometric errors.

(iv) Galaxy-galaxy interactions appear to have little (and perhaps no) effect on the optical colours of red galaxies in pairs. The slight reddening we detect at small separations (up to 0.015 mag in global and fibre colours) could be due to dust obscuration, but the rapid decline with pair separation and the absence of any difference between global and fibre colours instead suggest that residual problems with crowded-field photometry may be responsible.

(v) Unlike previous studies of close pairs, we find no significant excess ($< 1\%$) of extremely red galaxies in close pairs. We demonstrate that this is due to our improved photometry in crowded systems, given that we do find a strong excess ($\sim 6\%$) if we replace our GIM2D colours with Petrosian or modelMag colours from the SDSS database.

(vi) At a fixed global colour, blue cloud galaxies in close pairs have bluer fibre colours than control galaxies, with this difference decreasing as pair separation increases. No such difference is found for red galaxies at any separations.

(vii) Our simple starburst+galaxy model predicts that a 20% induced starburst should make a blue cloud (red sequence) galaxy bluer by about 0.05 mag (0.15 mag), and should persist for ~ 400 Myr before starting to diminish. Our observed colour offsets indicate that starbursts such as this are in fact found in blue cloud galaxies in pairs, but are absent in red sequence galaxies in pairs.

Together, these results provide further evidence that gas-rich galaxies in close pairs undergo induced star formation during close peri-centre passages, with the starburst then aging as the galaxies move apart from one another. Fibre colours confirm that this star formation is centrally concentrated, and measurements of projected local density show that this process occurs primarily in low- to medium-density environments. We find no evidence from optical colours for such induced star formation in red sequence galaxies, thereby confirming that any such star formation is likely to be obscured. We refute earlier claims of a substantial excess of extremely red galaxies in close pairs.

ACKNOWLEDGMENTS

We thank the anonymous referee for insightful comments which significantly improved this paper. We are grateful to Anja von der Linden and the MPA/JHU group for access to their data products and catalogues (maintained by Jarle Brinchmann at <http://www.mpa-garching.mpg.de/SDSS/>). We thank Ivan Baldry for making his DR7 projected local density measurements publicly available. SLE and DRP gratefully acknowledge the receipt of NSERC Discovery Grants which funded this research.

The SDSS is managed by the Astrophysical Research Consortium for the Participating Institutions. The Participating Institutions are the American Museum of Natural History, Astrophysical Institute Potsdam, University of Basel, University of Cambridge, Case Western Reserve University, University of Chicago, Drexel University, Fermilab, the Institute for Advanced Study, the Japan Participation Group, Johns Hopkins University, the Joint Institute for Nuclear Astrophysics, the Kavli Institute for Particle Astrophysics and Cosmology, the Korean Scientist Group, the Chinese

Academy of Sciences (LAMOST), Los Alamos National Laboratory, the Max-Planck-Institute for Astronomy (MPIA), the Max-Planck-Institute for Astrophysics (MPA), New Mexico State University, Ohio State University, University of Pittsburgh, University of Portsmouth, Princeton University, the United States Naval Observatory, and the University of Washington.

REFERENCES

- Abazajian, K. N., et al. 2009, *ApJS*, 182, 543
- Abbas, U., & Sheth, R. K. 2006, *MNRAS*, 372, 1749
- Alonso, M. S., Tissera, P. B., Coldwell, G., & Lambas, D. G. 2004, *MNRAS*, 352, 1081
- Baldry, I. K., Glazebrook, K., Brinkmann, J., Ivezić, Ž., Lupton, R. H., Nichol, R. C., & Szalay, A. S. 2004, *ApJ*, 600, 681
- Baldry, I. K., Balogh, M. L., Bower, R. G., Glazebrook, K., Nichol, R. C., Bamford, S. P., & Budavari, T. 2006, *MNRAS*, 373, 469
- Balogh, M. L., Baldry, I. K., Nichol, R., Miller, C., Bower, R., & Glazebrook, K. 2004, *ApJL*, 615, L101
- Barton, E. J., Geller, M. J., & Kenyon, S. J. 2000, *ApJ*, 530, 660
- Barton Gillespie, E., Geller, M. J., & Kenyon, S. J. 2003, *ApJ*, 582, 668
- Barton, E. J., Arnold, J. A., Zentner, A. R., Bullock, J. S., & Wechsler, R. H. 2007, *ApJ*, 671, 1538
- Bergvall, N., Laurikainen, E., & Aalto, S. 2003, *A&A*, 405, 31
- Blanton, M. R., & Roweis, S. 2007, *AJ*, 133, 734
- Brown, M. J. I., et al. 2009, *ApJ*, 703, 150
- Chen, Y., Lowenthal, J. D., & Yun, M. S. 2010, *ApJ*, 712, 1385
- Conselice, C. J., Chapman, S. C., & Windhorst, R. A. 2003, *ApJL*, 596, L5
- Cooper, M. C., et al. 2006, *MNRAS*, 370, 198
- Cox, T. J., Jonsson, P., Primack, J. R., & Somerville, R. S. 2006, *MNRAS*, 373, 1013
- Darg, D. W., et al. 2010, *MNRAS*, 401, 1552
- Dasyra, K. M., Yan, L., Helou, G., Surace, J., Sajina, A., & Colbert, J. 2008, *ApJ*, 680, 232
- De Propriis, R., Liske, J., Driver, S. P., Allen, P. D., & Cross, N. J. G. 2005, *AJ*, 130, 1516
- De Propriis, R., Conselice, C. J., Liske, J., Driver, S. P., Patton, D. R., Graham, A. W., & Allen, P. D. 2007, *ApJ*, 666, 212
- Deng, X.-F., He, J.-Z., Jiang, P., Song, J., & Tang, X.-X. 2008, *ApJ*, 677, 1040
- Di Matteo, P., Combes, F., Melchior, A.-L., & Semelin, B. 2007, *A&A*, 468, 61
- Di Matteo, P., Bournaud, F., Martig, M., Combes, F., Melchior, A.-L., & Semelin, B. 2008, *A&A*, 492, 31
- Ellison, S. L., Patton, D. R., Simard, L., & McConnachie, A. W. 2008, *AJ*, 135, 1877
- Ellison, S. L., Simard, L., Cowan, N. B., Baldry, I. K., Patton, D. R., & McConnachie, A. W. 2009, *MNRAS*, 396, 1257
- Ellison, S. L., Patton, D. R., Simard, L., McConnachie, A. W., Baldry, I. K., & Mendel, J. T. 2010, *MNRAS*, 407, 1514
- Faber, S. M., et al. 2007, *ApJ*, 665, 265
- Gallazzi, A., et al. 2009, *ApJ*, 690, 1883
- Geller, M. J., Kenyon, S. J., Barton, E. J., Jarrett, T. H., & Kewley, L. J. 2006, *AJ*, 132, 2243
- Goto, T., Yagi, M., & Yamauchi, C. 2008, *MNRAS*, 391, 700
- Green, P. J., Myers, A. D., Barkhouse, W. A., Mulchaey, J. S., Bennert, V. N., Cox, T. J., & Aldcroft, T. L. 2010, *ApJ*, 710, 1578
- Habergham, S. M., Anderson, J. P., & James, P. A. 2010, *ApJ*, 717, 342
- Heiderman, A., et al. 2009, *ApJ*, 705, 1433
- Holmberg, E. 1958, *Meddelanden fran Lunds Astronomiska Observatorium Serie II*, 136, 1
- Hopkins, P. F., Lidz, A., Hernquist, L., Coil, A. L., Myers, A. D., Cox, T. J., & Spergel, D. N. 2007, *ApJ*, 662, 110
- Hou, L. G., Wu, X.-B., & Han, J. L. 2009, *ApJ*, 704, 789
- Inami, H., et al. 2010, *AJ*, 140, 63
- Kannappan, S. J., Guie, J. M., & Baker, A. J. 2009, *AJ*, 138, 579
- Kauffmann, G., et al. 2003, *MNRAS*, 341, 33
- Kaviraj, S. 2010, *MNRAS*, 406, 382
- Kewley, L. J., Geller, M. J., & Barton, E. J. 2006, *AJ*, 131, 2004
- Knapen, J. H., & James, P. A. 2009, *ApJ*, 698, 1437
- Lambas, D. G., Tissera, P. B., Alonso, M. S., & Coldwell, G. 2003, *MNRAS*, 346, 1189
- Larson, R. B., & Tinsley, B. M. 1978, *ApJ*, 219, 46
- Leitherer, C., et al. 1999, *ApJS*, 123, 3
- Li, C., Kauffmann, G., Heckman, T. M., Jing, Y. P., & White, S. D. M. 2008, *MNRAS*, 385, 1903
- Lin, L., et al. 2008, *ApJ*, 681, 232
- Lin, L., et al. 2010, *ApJ*, 718, 1158
- López-Sanjuan, C., Balcells, M., Pérez-González, P. G., Barro, G., García-Dabó, C. E., Gallego, J., & Zamorano, J. 2010, *ApJ*, 710, 1170
- Lotz, J. M., Jonsson, P., Cox, T. J., & Primack, J. R. 2010, *MNRAS*, 404, 590
- Madau, P., Ferguson, H. C., Dickinson, M. E., Giavalisco, M., Steidel, C. C., & Fruchter, A. 1996, *MNRAS*, 283, 1388
- Martin, D. C., et al. 2007, *ApJS*, 173, 342
- Masjedi, M., et al. 2006, *ApJ*, 644, 54
- Masters, K. L., et al. 2010, *MNRAS*, 404, 792
- Mihos, J. C., & Hernquist, L. 1994, *ApJL*, 425, L13
- Nikolic, B., Cullen, H., & Alexander, P. 2004, *MNRAS*, 355, 874
- Nolan, L. A., Raychaudhury, S., & Kabán, A. 2007, *MNRAS*, 375, 381
- Oesch, P. A., et al. 2010, *ApJL*, 714, L47
- Owers, M. S., Blake, C., Couch, W. J., Pracy, M. B., & Bekki, K. 2007, *MNRAS*, 381, 494
- Park, C., & Choi, Y.-Y. 2009, *ApJ*, 691, 1828
- Patton, D. R., Pritchett, C. J., Yee, H. K. C., Ellingson, E., & Carlberg, R. G. 1997, *ApJ*, 475, 29
- Patton, D. R., Carlberg, R. G., Marzke, R. O., Pritchett, C. J., da Costa, L. N., & Pellegrini, P. S. 2000, *ApJ*, 536, 153
- Patton, D. R., et al. 2002, *ApJ*, 565, 208
- Patton, D. R., Grant, J. K., Simard, L., Pritchett, C. J., Carlberg, R. G., & Borne, K. D. 2005, *AJ*, 130, 2043
- Patton, D. R., & Atfield, J. E. 2008, *ApJ*, 685, 235
- Perez, M. J., Tissera, P. B., Scannapieco, C., Lambas, D. G., & de Rossi, M. E. 2006, *A&A*, 459, 361
- Perez, J., Tissera, P., & Blaizot, J. 2009a, *MNRAS*, 397, 748
- Perez, J., Tissera, P., Padilla, N., Alonso, M. S., & Lambas, D. G. 2009b, *MNRAS*, 399, 1157
- Pracy, M. B., Kuntschner, H., Couch, W. J., Blake, C., Bekki, K., & Briggs, F. 2009, *MNRAS*, 396, 1349
- Robaina, A. R., et al. 2009, *ApJ*, 704, 324
- Rogers, B., Ferreras, I., Kaviraj, S., Pasquali, A., & Sarzi, M. 2009, *MNRAS*, 399, 2172
- Rossa, J., Laine, S., van der Marel, R. P., Mihos, J. C., Hibbard, J. E., Böker, T., & Zabludoff, A. I. 2007, *AJ*, 134, 2124
- Ruhland, C., Bell, E. F., Häußler, B., Taylor, E. N., Barden, M., & McIntosh, D. H. 2009, *ApJ*, 695, 1058
- Rupke, D. S. N., Kewley, L. J., & Barnes, J. E. 2010, *ApJL*, 710, L156
- Salim, S., et al. 2007, *ApJS*, 173, 267
- Schimminovich, D., et al. 2007, *ApJS*, 173, 315
- Shi, Y., Rieke, G., Lotz, J., & Perez-Gonzalez, P. G. 2009, *ApJ*, 697, 1764
- Simard, L., et al. 2002, *ApJS*, 142, 1
- Simard, L., Patton, D. R., Ellison, S. L., J. Trevor Mendel, & McConnachie, A. W. 2010, *ApJS*, submitted
- Skelton, R. E., Bell, E. F., & Somerville, R. S. 2009, *ApJL*, 699, L9
- Sol Alonso, M., Lambas, D. G., Tissera, P., & Coldwell, G. 2006, *MNRAS*, 367, 1029
- Sol Alonso, M., Michel-Dansac, L., & Lambas, D. G. 2010, *A&A*, 514, A57
- Strauss, M. A., et al. 2002, *AJ*, 124, 1810
- Tacconi, L. J., et al. 2008, *ApJ*, 680, 246
- Tal, T., van Dokkum, P. G., Nelan, J., & Bezanson, R. 2009, *AJ*, 138, 1417
- Treister, E., Natarajan, P., Sanders, D. B., Urry, C. M., Schawinski, K., & Kartaltepe, J. 2010, *Science*, 328, 600

- Wang, J. L., Xia, X. Y., Mao, S., Cao, C., Wu, H., & Deng, Z. G. 2006, *ApJ*, 649, 722
- West, A. A., Garcia-Appadoo, D. A., Dalcanton, J. J., Disney, M. J., Rockosi, C. M., & Ivezić, Ž. 2009, *AJ*, 138, 796
- Whitaker, K. E., & van Dokkum, P. G. 2008, *ApJL*, 676, L105
- Wild, V., Walcher, C. J., Johansson, P. H., Tresse, L., Charlot, S., Pollo, A., Le Fèvre, O., & de Ravel, L. 2009, *MNRAS*, 395, 144
- Woods, D. F., Geller, M. J., & Barton, E. J. 2006, *AJ*, 132, 197
- Woods, D. F., & Geller, M. J. 2007, *AJ*, 134, 527
- Woods, D. F., Geller, M. J., Kurtz, M. J., Westra, E., Fabricant, D. G., & Dell'Antonio, I. 2010, *AJ*, 139, 1857
- Yamauchi, C., Yagi, M., & Goto, T. 2008, *MNRAS*, 390, 383
- Rodríguez Zaurín, J., Tadhunter, C. N., & González Delgado, R. M. 2010, *MNRAS*, 403, 1317
- Zhang, H.-X., Gao, Y., & Kong, X. 2010, *MNRAS*, 401, 1839